

LM-03K029  
March 20, 2003

---

---

## Immiscibility in the $\text{Fe}_3\text{O}_4\text{-FeCr}_2\text{O}_4$ Spinel Binary

S.E. Ziemniak, R.A. Castelli

---

---

### NOTICE

This report was prepared as an account of work sponsored by the United States Government. Neither the United States, nor the United States Department of Energy, nor any of their employees, nor any of their contractors, subcontractors, or their employees, makes any warranty, express or implied, or assumes any legal liability or responsibility for the accuracy, completeness or usefulness of any information, apparatus, product or process disclosed, or represents that its use would not infringe privately owned rights.

Immiscibility in the  
 $\text{Fe}_3\text{O}_4\text{-FeCr}_2\text{O}_4$  Spinel Binary

S. E. Ziemniak

R. A. Castelli

Lockheed Martin Corporation

P.O. Box 1072

Schenectady, New York 12301-1072

### ABSTRACT

A recent thermodynamic model of mixing in spinel binaries, based on changes in cation disordering ( $x$ ) between tetrahedral and octahedral sites (Ref. 1), is investigated for applicability to the  $\text{Fe}_3\text{O}_4\text{-FeCr}_2\text{O}_4$  system under conditions where incomplete mixing occurs. Poor agreement with measured consolute solution temperature and solvus (Ref. 2) is attributed to neglect of: (1) ordering of magnetic moments of cations in the tetrahedral sublattice antiparallel to the moments of those in the octahedral sublattice and (2) pair-wise electron hopping between octahedral site  $\text{Fe}^{3+}$  and  $\text{Fe}^{2+}$  ions. Disorder free energies ( $\Delta G_D$ ), from which free energies of mixing are calculated, are modeled by

$$\Delta G_D = \alpha x + \beta x^2 - T (S_c + x\sigma_{el} + \gamma x\sigma^{mag})$$

where the previously-neglected effects are accommodated by: (1) adding a non-configurational entropy term to provide coupling between cation disordering and magnetic ordering and (2) revising the configurational entropy ( $S_c$ ) analysis. Applying the constraint  $\alpha = -(2/3)\beta$  and regressing the existing database for  $\text{Fe}^{2+}$  ion disorder in  $\text{Fe}_3\text{O}_4$  gives:  $\beta = -31,020 \pm 1050 \text{ J mol}^{-1}$ ,  $\sigma_{el}/R = -0.730 \pm 0.081$  and  $\gamma$ , the coupling parameter between cation disordering and magnetic ordering,  $= -0.664 \pm 0.075$ . The revised mixing model predicts a consolute solution temperature ( $T_{cs}$ ) =  $600^\circ\text{C}$  and a solvus at  $500^\circ\text{C}$  of  $n = 0.05$  and  $0.70$  for the  $\text{Fe}(\text{Fe}_{1-n}\text{Cr}_n)_2\text{O}_4$  spinel binary.

## Immiscibility in the $\text{Fe}_3\text{O}_4\text{-FeCr}_2\text{O}_4$

### Spinel Binary

#### INTRODUCTION

Spinel is a double metal oxide ( $\text{AB}_2\text{O}_4$ ) which contains interstitial metal cations in lattice sites having two distinct types of symmetry with respect to the oxygen anions: tetrahedral and octahedral. Because the ratio of occupied octahedral-to-tetrahedral sites is 2/1, spinels with their B cations in octahedral sites (and A cations in tetrahedral sites) are classified as normal spinels. Those with their A cations only in octahedral sites are classified as inverse spinels. This distinction becomes important when solid solutions, formed by mixing two spinels that share a common A or B cation, are analyzed. Spinel binaries containing Fe, Ni and Cr are of practical importance because of their unique electric and magnetic properties and as their presence as corrosion oxides formed on alloys exposed to hydrothermal environments in electric power plants.

Spinel binaries formed by mixing two normal spinels (or two inverse spinels) are nearly ideal, and their analysis is straightforward. The mixing of a normal and an inverse spinel, however, results in non-ideal behavior and in certain instances, may result in immiscibility. For example, mixing studies of two inverse-normal spinel binaries,  $\text{Fe}(\text{Fe}_{1-n}\text{Cr}_n)_2\text{O}_4$  and  $\text{Ni}(\text{Fe}_{1-n}\text{Cr}_n)_2\text{O}_4$ , have demonstrated the existence of a consolute solution temperature ( $T_{cs}$ ) at 880 and 750°C, respectively. The solvus at 500°C was found to occur at  $n = 0.1, 0.7$  in the iron system (Ref. 2) and at  $n = 0.2, 0.7$  in the nickel system (Ref. 3). These results are supported by the corrosion

oxide layer(s) found on stainless steel exposed to high temperature water, i.e.,  $n = 0.05, 0.7$  (Ref. 4).

Recently, O'Neill and Navrotsky (Ref. 1) developed a thermodynamic model to calculate free energies of mixing in spinel binaries. The model was formulated by minimizing the free energy of disorder, in which disordering enthalpy is proportional to the square of the degree of disordering ( $x$ ) and disordering entropy is related to configurational entropy ( $S_c$ ) as determined by application of the Temkin equation (Ref. 5). The model successfully predicts  $\Delta G_{\text{mix}}$  in the  $\text{Fe}(\text{Fe}_{1-n}\text{Cr}_n)_2\text{O}_4$  spinel binary throughout the high temperature range where complete mixing occurs, i.e., 1000-1400°C. Application of the model at lower temperatures, as reported in Ref. 1, produced  $T_{\text{cs}} = 510^\circ\text{C}$  ( $n_{\text{cs}} = 0.40$ ) and a solvus at 300°C at  $n = 0.3, 0.8$ . These predictions deviate significantly from the measured values. Most of the deviation appears to be caused by neglect of a second type of ordering common in transition metal oxides, namely magnetic ordering between sublattices. By applying an alternate modeling approach (referred to as the compound energy model), which includes both types of ordering as well as contributions from sub-stoichiometry, lattice vacancy and interstitial ion effects, Taylor and Dinsdale (Ref. 6) predicted  $T_{\text{cs}} = 665^\circ\text{C}$  ( $n_{\text{cs}} = 0.40$ ) for the  $\text{Fe}_3\text{O}_4\text{-FeCr}_2\text{O}_4$  binary. More importantly, the solvus at 500°C was predicted to occur at  $n = 0.04, 0.76$ , in excellent agreement with the experimental measurements.

Due to these encouraging results, an effort is undertaken herein to 'repair' the Ref. 1 spinel mixing model. We note that Ref. 1 recognized that an additional term, namely non-configurational entropy, needed to be included when the spinels contained transition metal

cations. An electronic entropy term, arising from differences in crystal field stabilization entropy for a transition metal cation in an octahedral vs. a tetrahedral site, was recommended:

$$\sigma_{el} = \sigma_{CFS}(oct) - \sigma_{CFS}(tet)$$

However, the existing model does not account for two additional effects that occur in spinels containing iron ions: (1) magnetic ordering effects and (2) pair-wise electron hopping between octahedral site  $Fe^{3+}$  and  $Fe^{2+}$  ions. The first phenomenon is expected to impact non-configurational entropy, while the second alters the configurational entropy calculation. Recent advances in the formalism developed for quantifying magnetic contributions to the thermodynamic properties of transition metal oxides (Refs. 7-9) facilitate estimation of the former term.

#### MAGNETIC ORDERING CONTRIBUTION TO ENTROPY, $\sigma^{mag}$

Magnetic ordering in  $Fe_3O_4$  is known to cause the moments of the tetrahedral  $Fe^{3+}$  ions to align antiparallel to the moments of the octahedral  $Fe^{3+}$  and  $Fe^{2+}$  ions (Ref. 10). This type of magnetism is referred to as ferrimagnetism and occurs in magnetite at all temperatures  $< 850$  K (Ref. 11). The phenomenon is composition-dependent in the  $Fe(Fe_{1-n}Cr_n)_2O_4$  system: Curie temperatures decrease as  $n$  increases, so that solid solutions having  $n \geq 0.6$  become ferrimagnetic only below ambient temperature (Ref. 12). Since magnetic ordering exists in low  $n$  solutions and not in high  $n$  solutions in the temperature range of interest (573-850 K), it represents an asymmetric influence which may cause the solvus to depart asymmetrically from its point of initiation at  $T_{cs}$ .

Loss of magnetic ordering is accompanied by a decrease in heat capacity ( $C_p$ ) at the transformation temperature. The effect on thermodynamic properties is quantified by resolving the temperature functionality of  $C_p$  into magnetic and non-magnetic contributions and performing the proper integrations with respect to temperature to obtain  $\Delta H^{\text{mag}}$ ,  $\sigma^{\text{mag}}$  and  $\Delta G^{\text{mag}}$ . Inden (Ref. 13) first noted that the magnetic contribution to heat capacity,  $C_p^{\text{mag}}$ , followed a nearly universal behavior when scaled using dimensionless temperature,  $\tau = T/T_c$ . Here  $T_c$  is the critical temperature of magnetic ordering, i. e., Curie or Néel. For  $\tau < 1$   $C_p^{\text{mag}}$  was described by a logarithmic expression in  $\tau^3$  terms; for  $\tau > 1$  the logarithmic expression involved  $\tau^5$  terms. Since the derived expression for the magnetic contribution to entropy is very complicated, Hillert and Jarl (Ref. 14) developed a simplified approach to calculate  $\sigma^{\text{mag}}$  by expanding Inden's model into a series which was truncated after three terms:

for  $\tau \leq 1$

$$-\sigma^{\text{mag}} / R = \ln(\beta_m + 1) - \frac{\ln(\beta_m + 1)}{A} \left[ \left( \frac{474}{497} \right) \left( \frac{1}{p} - 1 \right) \right] \left[ \frac{4}{6} \tau^3 + \frac{10}{135} \tau^9 + \frac{16}{600} \tau^{15} \right]$$

and for  $\tau > 1$

$$-\sigma^{\text{mag}} / R = \frac{\ln(\beta_m + 1)}{A} \left[ \frac{4}{10} \tau^{-5} + \frac{14}{315} \tau^{-15} + \frac{24}{1500} \tau^{-25} \right]$$

where  $A = 518/1125 + (11692/15975) ((1/p) - 1)$

Model formalism provides the respective low and high temperature limits for  $-\sigma^{\text{mag}} / R$  as  $\ln(\beta_m + 1)$  and zero, and a different slope for  $d\sigma^{\text{mag}} / dT$  at  $T_c$  when approached from below or above  $T_c$ ; the two slopes differing by a factor of  $(474/497) (1/p - 1)$ , i.e., 2.452. The latter

behavior is a characteristic of the Inden model, which recognizes short-range magnetic ordering effects above the Curie temperature.

Application of the model requires the use of a common structural factor,  $p = 0.28$  for *fcc* phases, and end member values for  $\beta_m$  and  $T_c$ . For  $\text{Fe}_3\text{O}_4$ ,  $\beta_m = 44.54$  and  $T_c = 848$  K (Refs. 15, 16); those for  $\text{FeCr}_2\text{O}_4$  are  $\beta_m = 0.9$  and  $T_c = 100$  K (Ref. 6). Recent low temperature heat capacity measurements reported for  $\text{FeCr}_2\text{O}_4$  (Ref. 17), however, reveal that its magnetic ordering is more complex than modeled above. First, a  $C_p$  anomaly at 120 K results from a crystallographic transition (tetragonal-to-cubic) and is a non-magnetic effect. Second, two magnetic transitions are observed at lower temperatures:  $\sim 70$  K (Néel temperature) and  $\sim 35$  K. Below 35 K, a conical magnetic structure exists, while the spins are collinear between 35 and 70 K (Ref. 18). Although we resolved these inconsistencies by adjusting  $T_c$  for  $\text{FeCr}_2\text{O}_4$  to 71 K in the Ref. 6 correlation, a refit of the  $C_p$  data which includes the latest Ref. 17 measurements, and states how the non-magnetic  $C_p$  anomaly is treated, is warranted.

Curie temperatures for the spinel binary were described by fitting a third order Redlich-Kister polynomial to  $T_c(n)$  data provided in Ref. 12. The composition dependency of  $\beta_m$  was also modeled by a Redlich-Kister polynomial except that  $\ln(\beta_m + 1)$  was parameterized (rather than  $\beta_m$ ), as recommended by the Calphad group (Ref. 9). Only linear terms were retained, due to lack of data:

$$T_c(n) = 71n + 848(1-n) - 234.7n(1-n) - 527.8n(1-n)(2n-1)$$

and



$$\ln (\beta_m(n) + 1) = 0.6419 n + 3.8186 (1-n)$$

Estimated Curie temperatures deviated from the Ref. 12 measurements by  $\pm 19$  K ( $1\sigma$ ).

As shown in Fig. 1, the magnetic contribution to entropy in the  $\text{Fe}(\text{Fe}_{1-n}\text{Cr}_n)_2\text{O}_4$  binary is negligible at room temperature for solids having  $n > 0.6$  and for all solids above  $1000^\circ\text{C}$ .

### LATTICE PARAMETER ANALYSIS

On the basis of powder X-ray diffraction measurements provided by JCPDS (Ref. 19), unit cell dimensions for magnetite (inverse spinel) and chromite (normal spinel) are given as  $8.396 \text{ \AA}$  and  $8.376 \text{ \AA}$ , respectively. Lattice parameters for the spinel binary  $\text{Fe}(\text{Fe}_{1-n}\text{Cr}_n)_2\text{O}_4$  are available from the earlier investigations of Yearian et al. (Ref. 20) and Robbins et al. (Ref. 12). The results of Ref. 12 are especially valuable because they provide independent determinations of the distribution of  $\text{Fe}^{3+}$  and  $\text{Fe}^{2+}$  ions between octahedral and tetrahedral sites by Mossbauer spectroscopy.

Based on known geometric relationships for a cubic, close-packed arrangement of oxygen ions, the interatomic (M-O) distance between a tetrahedral metal ion and its nearest oxygen ion neighbors is given by (Ref. 21):

$$\text{tet bond length} = a_o \sqrt{3} (u - 1/8)$$

and that between an octahedral metal ion and its nearest oxygen ion neighbors is given by

$$\text{oct bond length} = a_0 (3u^2 - 2u - 3/8)^{1/2}$$

where  $a_0$  is the lattice parameter and  $u$  is an oxygen positional parameter. The latter is a measure of lattice distortion caused by size differences between metal cations. The above two relationships allow lattice parameters to be determined from cation sizes, since sizes of the oxygen ions are known, see Table I. By linking the spinel geometrical relationships with the measured lattice parameters and Mossbauer-based cation distributions, an internal consistency check on cation sizes is obtained.

As shown in Fig. 2, lattice parameters in the  $\text{Fe}(\text{Fe}_{1-n}\text{Cr}_n)_2\text{O}_4$  binary vary linearly with  $n$  in a zigzag manner; three distinct crystallographic regions being observed: (1) Region I ( $0 \leq n \leq 1/3$ ), (2) Region II ( $1/3 \leq n \leq 2/3$ ) and (3) Region III ( $2/3 \leq n \leq 1$ ). The analysis of the chromite-rich region is the most straightforward since  $\text{Fe}^{3+}$  ions are present only on octahedral sites. Therefore,  $\text{Cr}^{3+}$  ion substitution for  $\text{Fe}^{3+}$  occurs only on octahedral sites. The cation distribution pattern is written

	<u>Ion</u>	<u>Tet</u>	<u>Oct</u>	<u>Sum</u>
	$\text{Fe}^{2+}$	1	0	1
Region III	$\text{Fe}^{3+}$	0	$2-2n$	$2-2n$
$(2/3 \leq n \leq 1)$	$\text{Cr}^{3+}$	<u>0</u>	<u><math>2n</math></u>	<u><math>2n</math></u>
	Sum	1	2	3

On the basis of ion sizes recommended by Shannon (Ref. 22) for  $\text{Cr}^{3+}(\text{oct})$  and oxygen, the lattice parameters in Region III provide  $\text{Fe}^{3+}(\text{oct}) = 0.65 \text{ \AA}$  and  $\text{Fe}^{2+}(\text{tet}) = 0.576 \text{ \AA}$ . Although the ionic radius for  $\text{Fe}^{3+}(\text{oct})$  agrees with the Ref. 22 value of  $0.645 \text{ \AA}$ , our calculated radius for  $\text{Fe}^{2+}(\text{tet})$  is significantly smaller than that recommended by Ref. 22 (i.e.,  $0.63$ ).

On the other hand, initial  $\text{Cr}^{3+}$  ion substitution in the ferrite-rich region displaces equal amounts of  $\text{Fe}^{3+}$  and  $\text{Fe}^{2+}$  ions from octahedral sites, so that  $\text{Fe}^{2+}$  ions begin to appear on tetrahedral sites.

The cation distribution is given by

	<u>Ion</u>	<u>Tet</u>	<u>Oct</u>	<u>Sum</u>
	$\text{Fe}^{2+}$	$n$	$1-n$	$1$
Region I	$\text{Fe}^{3+}$	$1-n$	$1-n$	$2-2n$
$(0 \leq n \leq 1/3)$	$\text{Cr}^{3+}$	$0$	$2n$	$2n$
	Sum	$1$	$2$	$3$

It is known (Refs. 23, 24) that a rapid electron exchange reaction occurs between octahedral  $\text{Fe}^{3+}$  and  $\text{Fe}^{2+}$  ions in magnetite ( $n = 0$ ), so that the two ions become (nearly) indistinguishable. The electron "hopping" phenomenon continues into the ferrite-rich region such that equal amounts of  $\text{Fe}^{3+}$  and  $\text{Fe}^{2+}$  ions are retained on the octahedral sites. Such behavior indicates that electron hopping occurs in a pair-wise manner. Upon retaining the cation sizes consistent with Region III, the Region I lattice parameters provide an ionic radius for indistinguishable  $\text{Fe}^{3+}/\text{Fe}^{2+}$  ion pairs in octahedral sites that exhibit electron exchange as  $0.666 \text{ \AA}$ .

Finally, in Region II it is no longer possible to retain equal amounts of  $\text{Fe}^{3+}$  and  $\text{Fe}^{2+}$  ions on octahedral sites. This change is accounted for by retaining the pair-hopping concept but allowing the excess  $\text{Fe}^{3+}$  ions on octahedral sites to appear as distinguishable entities. The cation distribution pattern is summarized as

	<u>Ion</u>	<u>Tet</u>	<u>Oct<sub>1</sub></u>	<u>Oct<sub>2</sub></u>	<u>Sum</u>
	$\text{Fe}^{2+}$	$2n-1/3$	$4/3-2n$	-	1
Region II	$\text{Fe}^{3+}$	$4/3-2n$	$4/3-2n$	$2n-2/3$	$2-2n$
$1/3 \leq n \leq 2/3$	$\text{Cr}^{3+}$	<u>0</u>	<u>2n</u>	-	<u>2n</u>
	Sum	1	2		3

By retaining all of the iron ion radii determined from the lattice parameter analyses of Regions I and III, except for the indistinguishable  $\text{Fe}^{3+}/\text{Fe}^{2+}$  ion octahedral pairs, a lattice parameter analysis of Region II provides an additional estimate as 0.666 Å. This value is identical to that determined previously and demonstrates the desired internal consistency.

In summary, the observed lattice parameter dependency of the  $\text{Fe}(\text{Fe}_{1-n}\text{Cr}_n)_2\text{O}_4$  binary on composition ( $n$ ) is shown to be consistent with the ion sizes summarized in Table I and the quantified cation distribution patterns for three distinct crystallographic regions given in this section. Results of the various bond length calculations are summarized in Fig. 2. Thus, independent of a thermodynamic model to predict cation disordering, the fraction of divalent, tetrahedral cations displaced to octahedral sites (at room temperature) is given by  $1-n$ ,  $4/3 - 2n$  and 0 for the respective Regions I, II and III.

### FREE ENERGIES OF MIXING

Consistent with the analysis of O'Neill and Navrotsky (Ref. 1), a spinel disordering parameter  $x$  is defined to represent the fraction of divalent, tetrahedral cations displaced to octahedral sites.

The change in free energy due to cation disordering is given by

$$\Delta G_D = \alpha x + \beta x^2 - T [S_c + \sigma x]$$

where  $S_c$  is the configurational entropy of the equilibrium arrangement,  $\sigma$  is a non-configurational entropy term and  $x$  is determined from the  $\alpha$  and  $\beta$  parameters associated with the change in non-configurational enthalpy which satisfies the equilibrium cation arrangement formulated by setting

$$\frac{\partial \Delta G_D}{\partial x} = 0$$

Configurational entropy is calculable for spinels, which have multiple cation sites, by application of the Temkin equation (Ref. 5):

$$-S_c / R = \sum b_s (m_i \ln m_i)_s$$

where  $m_i$  is the mole fraction of component  $i$  on site  $s$ . Each spinel has three lattice sites per formula unit:  $b_s = 1$  for tetrahedral and  $b_s = 2$  for octahedral. For example, substitution of the cation distribution for a normal spinel,  $\text{FeCr}_2\text{O}_4$  ( $n = 1$ ), into the Temkin equation gives  $-S_c / R = 0$ , while the inverted configuration of  $\text{Fe}_3\text{O}_4$  ( $n = 0$ ) provides  $-S_c / R = -2 \ln 2$ .

The O'Neill-Navrotsky methodology is applied in two stages: (1) determine  $x$  for both pure component, end-member spinels  $\text{Fe}_3\text{O}_4$  ( $n = 0$ ) and  $\text{FeCr}_2\text{O}_4$  ( $n = 1$ ), followed by (2) determination of  $x$  for the solid solution. Free energies of mixing follow from differences in  $\Delta G_D$  between the solid solution and mol fraction-weighted contributions of the end-member solids using a regular solution model:

$$\Delta G_{mix} = W n (1-n) + \Delta G_D^{mix}$$

where  $\Delta G_D^{mix} = \Delta G_D(n) - [n \Delta G_D(n=1) + (1-n) \Delta G_D(n=0)]$  and  $W$  is the (temperature-invariant) regular solution parameter for the  $\text{Fe}(\text{Fe}_{1-n}\text{Cr}_n)_2\text{O}_4$  binary. The effect of unpaired electrons has been incorporated into the  $\Delta G_D^{mix}$  calculation to avoid writing a separate  $\Delta G_{el}^{mix}$  term, i.e.,  $\sigma = \sigma_{el}$ .  $\sigma_{el}$  is non-zero for spinels that contain transition metal ions.

Presently, two additional model corrections are necessary to account for: (1) octahedral site electron hopping which modifies the  $S_C$  analysis and (2) magnetic ordering between the octahedral and tetrahedral sublattices which causes a coupling between cation disordering and magnetic ordering. With regard to the first, it is noted that the modeling parameters that describe the enthalpy of disordering in magnetite ( $\alpha$ ,  $\beta$ ) are presently based on the Ref. 1 analysis that does not consider electron hopping. When pair-wise hopping is recognized, the revised cation distribution for  $\text{Fe}_3\text{O}_4$  is written:

<u>Ion</u>	<u>Tet</u>	<u>Oct<sub>1</sub></u>	<u>Oct<sub>2</sub></u>	<u>Sum</u>
Fe <sup>2+</sup>	1-x	x	-	1
Fe <sup>3+</sup>	<u>x</u>	<u>x</u>	<u>2-2x</u>	<u>2</u>
Sum	1	2		3

The disordering analysis gives

$$-S_c / R = 3x \ln x + 3(1-x) \ln (1-x) - 2x \ln 2$$

while the equilibrium analysis allows x to be determined from

$$-RT \ln \frac{x^3}{(1-x)^3} = \alpha + 2\beta x - \sigma T - 2 RT \ln 2$$

In this manner, it is seen that electron hopping introduces the equivalent of an excess entropy term ( $2R \ln 2$ ) into the disordering equilibrium and changes the form of its logarithmic term.

Inclusion of an excess, or non-configurational, entropy term in the defining equation for  $\Delta G_D$  was originally recommended by O'Neill and Navrotsky for applications involving transition metal ions where electronic entropy effects are important. This contribution arises from crystal field stabilization effects experienced by cations in octahedral vs. tetrahedral sites having unpaired 3d electrons, and is readily calculated, i.e.,  $\sigma_{el} = -R \ln 2$  for  $\text{Fe}_3\text{O}_4$  (see Ref. 1, Appendix). Since magnetic ordering entropy interacts with the disordering equilibrium in a manner similar to electronic entropy, we believe that inclusion of  $\sigma^{mag}$  in  $\sigma$  will allow the effects of configurational disordering and magnetic ordering to be coupled.

Therefore, to complete revision of the  $\Delta G_D$  model, while allowing for coupling between configurational and magnetic ordering,  $\sigma$  is replaced in the above by  $\sigma_{el} + \gamma\sigma^{mag}$  to give

$$\Delta G_D = \alpha x + \beta x^2 - T (S_C + x\sigma_{el} + \gamma x\sigma^{mag})$$

The coupling parameter,  $\gamma$ , is expected to be a constant, similar to  $\alpha$  and  $\beta$ .

It is noted that a similar correction has been obtained by applying the Landau theory of phase transitions to cation ordering ( $Q$ ) and magnetic ordering ( $Q_m$ ) in spinels (Ref. 25). The ordering and disordering parameters are related by  $x = 2/3 (1-Q)$ . The lowest order coupling between the two processes is linear in  $Q$  ( $\propto x$ ) and quadratic in  $Q_m$  ( $\propto \sigma^{mag}$ ); the coupling term being expressed as  $\lambda Q Q_m^2$  (i.e.,  $\gamma x \sigma^{mag}$ ). The analysis of Harrison and Putnis (Ref. 25) is especially significant because it provides an estimate of  $x(T)$  for  $Fe_3O_4$  at temperatures below  $T_c$ . It also demonstrates that coupling does not appreciably affect magnetic ordering.

Results of a non-linear regression analysis of the  $x(T)$  database for magnetite, as represented by the measurements of Wu and Mason (Ref. 26), Nell, Wood and Mason (Ref. 27) and the low temperature estimates of Harrison and Putnis (Ref. 25), are shown in Fig. 3. The fitted parameters are provided in Table II. To facilitate comparisons with previous work, results of regression analyses are provided for cases where electron hopping is neglected. In this manner, it is seen that inclusion of  $\sigma_{el}$  (and  $\sigma^{mag}$  coupling) creates the inequality  $\alpha < \beta$  and allows the  $x$ -value approached in the high temperature limit to become  $< 2/3$ . Because the  $x(T)$  database is



mathematically inconsistent with an  $x = 2/3$  high temperature asymptote, it is important to include the entire  $x(T)$  database when fitting  $\alpha$ ,  $\beta$  and  $\gamma$ . The assumption that disordering of  $\text{Fe}_3\text{O}_4$  ( $\sigma_{el} \neq 0$ ) and  $\text{MgFe}_2\text{O}_4$  ( $\sigma_{el} = 0$ ) is identical, as applied by Harrison and Putnis, is inappropriate at high temperatures and explains why Ref. 25 had to truncate their non-convergent ordering analysis below  $1050^\circ\text{C}$  when fitting parameters to the Landau model.

Sensitivity of  $\Delta H_D$  to the  $\sigma_{el}$  constraint was investigated by performing three additional fits of  $\alpha$ ,  $\beta$  and  $\gamma$ : (1) constrain  $\sigma_{el}$  to  $-0.405R$  per Table III, (2)  $\sigma_{el} = 0$  and (3) constrain  $\Delta H_D$  to zero at  $x = 2/3$  (the random configuration) and fit  $\sigma_{el}$ . The third option is suggested to eliminate the constraint on  $\sigma_{el}$  and replace it with a generic link between stability of an inverse configuration and exothermicity of the disordering reaction. All four regression analyses provide equally good (and statistically significant) fits to the database.

Figure 4 compares the fitted disordering enthalpies for magnetite and confirms a high degree of correlation between  $\Delta H_D$  and  $\sigma_{el}$ . It is noted that a previous, less rigorous disordering model proposed by Navrotsky and Kleppa (Ref. 28) (incorrectly) assumed that  $\Delta H_D$  varied linearly with  $x$  and neglected  $\sigma_{el}$ .  $\Delta H_D$  (@  $x = 1$ ) was determined by differences in octahedral site preference energies (OSPE) for the two cations in the spinel:

$$\Delta H_D (@x = 1) = OSPE(A^{2+}) - OSPE(B^{3+})$$

To the same degree of approximation, Table III compares OSPEs derived from crystal field theory (Ref. 29) with changes in electronic entropy for the same cations in going from octahedral to tetrahedral coordination (Ref. 1, Table 4). For magnetite, the value  $\Delta H_D = -16.6 \text{ kJ mol}^{-1}$  is seen to be consistent with  $\sigma_{el} = -0.405R$ . Since the constraints  $\sigma_{el} = -R \ln 2$  or  $\alpha = -(2/3)\beta$  result in exothermic  $\Delta H_D$  values for  $\text{Fe}_3\text{O}_4$  that are closest to the Table III predictions, they represent the preferred options.

The disordering analysis for the other end-member,  $\text{FeCr}_2\text{O}_4$ , remains unchanged from Ref. 1. Due to high octahedral site preference energies (OSPE) exhibited by the  $\text{Cr}^{3+}$  ion, its disordering parameter remains negligibly small, regardless of temperature. This result allows disordering of  $\text{FeCr}_2\text{O}_4$  to be neglected, so only one disordering parameter is required to express the cation distribution in the  $\text{Fe}_3\text{O}_4$ - $\text{FeCr}_2\text{O}_4$  spinel binary:

	<u>Ion</u>	<u>Tet</u>	<u>Oct<sub>1</sub></u>	<u>Oct<sub>2</sub></u>	<u>Sum</u>
	$\text{Fe}^{2+}$	1-x	x	-	1
Region IH	$\text{Fe}^{3+}$	x	x	2-2n-2x	2-2n
$0 \leq n \leq 1$	$\text{Cr}^{3+}$	0	<u>2n</u>	-	<u>2n</u>
	Sum	1	2		3

The disordering analysis yields

$$-S_c / R = 3x \ln x + (1-x) \ln (1-x) + 2n \ln n + 2(1-n-x) \ln (1-n-x) - 2x \ln 2$$

with  $x$  to be determined from

$$-RT \ln \frac{x^3}{(1-x)(1-n-x)^2} = \alpha + 2\beta x - \sigma_{el}T - \gamma\sigma^{mag}(n)T - 2RT \ln 2$$

It is noted that the above equations reduce to those for magnetite in the  $n = 0$  limit. Solving the above equations for  $x$  provides the  $x(n, T)$  curves presented in Fig. 5. Above the Curie temperature for  $\text{Fe}_3\text{O}_4$ , all  $x(n)$  curves are seen to intersect at a common point  $(x_i, n_i)$  given by the solution to

$$\alpha + 2\beta x_i = 0 \quad \Rightarrow x_i = 0.333$$

and

$$\frac{x_i^3}{(1-x_i)(1-n_i-x_i)^2} = 1.928 \quad \Rightarrow n_i = 0.497$$

For the option  $\alpha = -(2/3)\beta$ . The alternate constraint,  $\sigma_{el} = -R \ln 2$ , provides a less favorable  $(x_i, n_i) = (0.360, 0.449)$ . In the high temperature limit,  $x(n)$  varies nearly linearly between its two end-points for  $\text{Fe}_3\text{O}_4$  ( $x \approx 2/3$ ) and  $\text{FeCr}_2\text{O}_4$  ( $x = 0$ ). It is noted that the calculated  $x(n, 1000)$  curve is virtually coincident with that calculated by Taylor and Dunsdale (Ref. 6) using the compound energy model. As temperatures approach the Curie temperature for  $\text{Fe}_3\text{O}_4$ , magnetic coupling becomes important and the  $x(n)$  curves develop a spinodal shape. The inverse spinel region expands at lower temperatures, and in the room temperature limit,  $\text{Fe}^{2+}$  ion disordering is described by  $x = 1-n$ . Likewise, the normal spinel region expands at lower temperatures, with  $x \rightarrow 0$  in the room temperature limit.

Plotted for comparison in Fig. 5 are the  $x$ -values derived from the (room temperature) lattice parameter analysis. It is seen that the predicted and inferred  $x$ -values at room temperature are in exact agreement at  $n = 0.55$  and  $n < 1/3$  but deviate by  $< 0.05$  for  $n > 2/3$ . The predicted  $x$ -values in proximity to  $n = 0.5$ , however, undergo a nearly stepwise change over a very small  $n$ -interval (i.e., 0.01). It is not known whether the discrepancy is due to a modeling deficiency or a non-equilibrium condition in the room temperature data. Nevertheless, a portion of the deviation occurs in a region where the disordering analysis may lose its validity, i.e., when  $n$  exceeds an upper limit ( $ul$ ) where  $Cr^{3+}$  ions dominate octahedral sites and octahedral  $Fe^{2+}$  ion concentrations approach zero. This limit was previously defined at room temperature as  $ul = 2/3$  (Region III).

Recent electrical conductivity measurements of the  $Fe(Fe_{1-n}Cr_n)_2O_4$  binary at elevated temperatures (Ref. 30) have demonstrated consistency with pair-wise electron hopping. For compositions  $n > 2/3$ , however, a nearly stepwise increase in activation energy for electron hopping was found to occur. Since the nearest neighbors of most octahedral  $Fe^{2+}$  ions are now  $Cr^{3+}$  ions (and no effect is observed when  $Cr^{3+}$  is replaced by  $Al^{3+}$ ), Nell and Wood (Ref. 30) concluded that the increased activation energy may represent hopping between  $Fe^{2+}$  and  $Fe^{3+}$  via  $Cr^{3+}$ . Given this new hopping vision, it is not obvious whether electron hopping will continue to involve pairs of octahedral  $Fe^{3+}$  and  $Fe^{2+}$  ions, or whether all octahedral  $Fe^{3+}$  will now become involved in hopping. To simplify our analysis we chose not to attempt further model revisions and took  $ul = 1$ .

Plots of  $\Delta G_{mix}$ , obtained by substituting  $\Delta G_D^{mix}$  calculated using  $x(n)$  from Fig. 5 into the O'Neill-Navrotsky model, are shown in Figs. 6a/b. Figure 6a compares predicted free energies

of mixing for the  $\text{Fe}(\text{Fe}_{1-n}\text{Cr}_n)_2\text{O}_4$  spinel binary at temperatures above  $1000^\circ\text{C}$  with the measurements of Snethlage and Schröcke (Ref. 31) and Petric and Jacob (Ref. 32). Excellent agreement is observed, provided that the regular solution parameter ( $W$ ) is selected as  $6500 \text{ J mol}^{-1}$ . At lower temperatures, the  $\Delta G_{\text{mix}}$  curves develop composition-dependent inflections, indicative of immiscibility. As shown in Fig. 6b the inflections are present only below  $880 \text{ K}$ . Further decreases in temperature lead to development of two localized minima, and  $\Delta G_{\text{mix}}$  first becomes positive at  $820 \text{ K}$  (near  $n \approx 0.1$ ).

Fig. 7 summarizes the solvus determined by constructing a common tangent to each  $\Delta G_{\text{mix}}$  curve. It is seen that the ferrite-rich solvus calculation has improved significantly compared to the Ref. 1 results where the effects of magnetic ordering and electron hopping were not considered. The solvus measurements of Cremer, when extrapolated to the temperature range  $300\text{-}500^\circ\text{C}$ , are seen to agree with the present predictions, those of Taylor and Dinsdale and the outer layer corrosion oxide formed on stainless steel during exposure to high temperature water. Although the chromite-rich solvus in the same temperature range is consistent with an extrapolation of Cremer's measurements and Taylor and Dinsdale's predictions, the chromite content is slightly over-predicted relative to that found in naturally-occurring minerals at  $450^\circ\text{C}$  and the inner layer composition of stainless steel corrosion films near  $300^\circ\text{C}$ . Less accurate model calculations were expected at  $n > 2/3$ , due to a change in the electron hopping phenomenon, which was not modeled.

## SUMMARY

The thermodynamics of mixing in a spinel binary has been investigated by applying four concepts to address deviations from ideality: (1) a regular solution model, (2) configurational entropy calculations to describe changes in cation disordering between tetrahedral and octahedral sites, (3) pairwise electron hopping between  $\text{Fe}^{3+}$  and  $\text{Fe}^{2+}$  ions in octahedral sites and (4) thermodynamic effects caused by magnetic ordering between cations in the tetrahedral and octahedral sublattices. Free energies of mixing are additive:

$$\Delta G_{mix} = W n(1-n) + \Delta G_D^{mix}$$

where  $\Delta G_D^{mix} = \Delta G_D(n) - [n \Delta G_D(n=1) + (1-n) \Delta G_D(n=0)]$  and  $W$  is the (temperature-invariant) regular solution parameter. In the absence of magnetic effects, O'Neill and Navrotsky (Ref. 1) predicted that mixing would be complete in the  $\text{Fe}_3\text{O}_4$ - $\text{FeCr}_2\text{O}_4$  binary at high temperatures ( $>900^\circ\text{C}$ ) and showed that the predicted free energies of mixing compared favorably with experimental measurements. Application of the mixing model at lower temperatures predicted immiscibility, although discrepant estimates were obtained for the solvus and consolute solution temperature.

Below the Curie temperature, magnetic ordering in  $\text{Fe}_3\text{O}_4$  causes the moments of the tetrahedral  $\text{Fe}^{3+}$  ions to align antiparallel to the moments of the octahedral  $\text{Fe}^{3+}$  and  $\text{Fe}^{2+}$  ions (Ref. 10). This type of magnetism is known as ferrimagnetism and exists in  $\text{Fe}_3\text{O}_4$  at temperatures below 850 K (Ref. 11). Curie temperatures decrease in the  $\text{Fe}(\text{Fe}_{1-n}\text{Cr}_n)_2\text{O}_4$  binary as  $n$  increases, so that solid solutions having  $n \geq 0.65$  are ferrimagnetic only below ambient temperature (Ref. 12). Since magnetic ordering exists in most high  $n$  solutions and not in low  $n$  solutions in the temperature range of interest (500-800 K), an asymmetric correction to the O'Neill-Navrotsky regular

solution model is provided which causes it to behave like a subregular solution model having a temperature-dependent coefficient at temperatures  $< T_c$ .

Free energy changes due to cation disordering from tetrahedral to octahedral sites are modeled by:

$$\Delta G_D = \alpha x + \beta x^2 - T(S_c + x\sigma_{el} + \gamma x\sigma^{mag})$$

By creating a disordering model containing a coupled magnetic ordering entropy term assures that cation disordering analyses will be compatible with cation ordering analyses based on Landau theory. An added benefit of the proposed disordering model is that it also contains a built-in feature to account for short-range magnetic ordering above  $T_c$ , which eliminates a weakness exhibited by Landau ordering analyses. Although our analysis relies on the Inden model to determine the magnetic contribution to entropy, it is noted that the Inden model was originally developed for use with metals that contain only one magnetic atom per formula unit. Therefore, applicability of the relationships to *fcc* metal oxides remains to be verified. Furthermore, no attempt was made to relate the resulting  $\beta_m$  value for  $Fe_3O_4$  to magnetic moments of its constituent ions. Thus, additional work remains to eliminate these modeling uncertainties.

An additional modeling feature, unique to spinels containing  $Fe^{3+}$  and  $Fe^{2+}$  ions, is imbedded in the calculation of disordering entropy: electron hopping between  $Fe^{3+}$  and  $Fe^{2+}$  ion pairs in octahedral sites. Because the rapid electron exchange occurs in a pairwise manner, a second, distinguishable type of octahedral  $Fe^{3+}$  ion (i.e., unpaired) is created. As demonstrated herein,

the phenomenon alters the configurational entropy calculation and requires the  $\alpha$  and  $\beta$  parameters to be refitted. Accounting for the thermodynamic effects of electron hopping increases  $T_{cs}$  in the  $\text{Fe}_3\text{O}_4$ - $\text{FeCr}_2\text{O}_4$  binary from  $510^\circ\text{C}$  to  $600^\circ\text{C}$ .

In closing, it is noted that the present mixing model adjustments introduce a minimum of adjustable parameters, i.e., one. When applied with three other model parameters ( $\alpha$ ,  $\beta$  and  $\sigma_{el}$ ), accurate  $\Delta G_{mix}$  predictions may be obtained in spinel binaries over a much broader range of temperature than has been demonstrated using other mixing models that possess many more adjustable parameters: up to 8 in Landau theory (Ref. 25) and up to 30 in the compound energy model (Ref. 5). Due to the high degree of correlation between model parameters, it is recommended that a constraint be imposed on  $\alpha$  and  $\beta$  which allows  $\Delta H_D < 0$  for stable inverse configurations and  $\Delta H_D > 0$  for normal configurations, rather than fixing  $\beta = -20.0 \text{ kJ mol}^{-1}$  as recommended by Ref. 1.



## REFERENCES

1. H. St. C. O'Neill and A. Navrotsky, *Amer. Mineral.* 68, 181 (1983) and 69, 733 (1984)
2. V. Cremer, *N. Jb. Miner. Abh.* 111, 184 (1969)
3. S.E. Ziemniak, A.R. Gaddipati and P.C. Sander, submitted
4. S.E. Ziemniak and M. Hanson, *Corros. Sci.* 44, 2209 (2002)
5. M. Temkin, *Acta Physicochim. URSS* 20, 411 (1945)
6. J. R. Taylor and A. T. Dinsdale, *Z. Metallkd.* 84, 335 (1993)
7. D. de Fontaine, S. G. Fries, G. Inden, P. Miodownik, R. Schmid-Fetzer and S.-L. Chen, *Calphad* 19, 499 (1995)
8. M. Hillert, B. Burton, S. K. Saxena, S. Degterov, K. C. Hari Kumar, H. Ohtani, F. Aldinger and A. Kussmaul, *CALPHAD* 21, 247 (1997)
9. I. Ansara, B. Burton, Q. Chen, M. Hillert, A. Fernandez-Guillermet, S. G. Fries, H. L. Lukas, H. J. Seifert and W. A. Oates, *CALPHAD* 24, 19 (2000)
10. L. Néel, *Ann. Phys. (Paris)* 3, 137 (1948)
11. F. van der Woude, G. A. Sawatzky and A.H. Morrish, *Phys. Rev.* 167, 533 (1968)
12. M. Robbins, G.K. Wertheim, R.C. Sherwood and D.N.E. Buchanan, *J. Phys. Chem. Solids* 32, 717 (1971)
13. G. Inden, *Z. Metallkd.* 66, 577 (1975)
14. M. Hillert and M. Jarl, *CALPHAD* 2, 227 (1978)
15. F. Grønvold and A. Sveen, *J. Chem. Thermo.* 6, 859 (1974)
16. B. Sundman, *J. Phase Eq.* 12, 127 (1991)
17. S. Klemme, H. St. C. O'Neill, W. Schnelle and E. Gmelin, *Amer. Mineral.* 85, 1686 (2000)

18. G. Shirane, D. Cox and S. Pickard, *J. Appl. Phys.* 35, 954 (1964)
19. JCPDS Powder Diffraction File, International Centre for Diffraction Data, Swarthmore, PA, 1989; Sets 1-39
20. H.J. Yearian, J.M. Kortright and R.H. Langenheim, *J. Chem. Phys.* 22, 1196 (1954)
21. R.J. Hill, J.R. Craig and G.V. Gibbs, *Phys. Chem. Minerals* 4, 317 (1979)
22. R.D. Shannon, *Acta Crystallog.* A32, 751 (1976)
23. E.J.W. Verwey, P.H. Haayman and F.C. Romeijn, *J. Chem. Phys.* 15, 181 (1947)
24. J.M. Daniels and A. Rosencwaig, *J. Phys. Chem. Solids* 30, 1561 (1969)
25. R. J. Harrison and A. Putnis, *Eur. J. Mineral.* 9, 1115 (1997)
26. C.C. Wu and T.O. Mason, *J. Amer. Ceramic Soc.* 64, 520 (1981)
27. J. Nell, B. J. Wood and T. O. Mason, *Amer. Mineral.* 74, 339 (1989)
28. A. Navrotsky and O. J. Kleppa, *J. Inorg. Nucl. Chem.* 29, 2701 (1967)
29. J. D. Dunitz and L. E. Orgel, *J. Phys. Chem. Solids* 3, 318 (1957)
30. J. Nell and B. J. Wood, *Amer. Mineral.* 76, 405 (1991)
31. R. Sneath and H. Schröcke, *N. Jb. Miner. Mh.* 5, 214 (1976)
32. A. Petric and K. T. Jacob, *J. Amer. Ceram. Soc.* 65, 117 (1982)

Table I

## Ionic Radii in Spinel,\* Å

<u>Ion</u>	<u>Tet.</u>	<u>Oct.</u>	
Fe <sup>2+</sup>	0.58	n.a.	} 0.666**
Fe <sup>3+</sup>	(0.49)	0.64	
Cr <sup>3+</sup>	--	(0.615)	
O <sup>2-</sup>	(1.38)	(1.40)	

---

\* Values in parentheses are taken from Ref. 22.

\*\* Value for indistinguishable Fe<sup>3+</sup> - Fe<sup>2+</sup> ion pairs linked by electron exchange reaction.

**Table II**  
**Thermodynamic Parameters Required to Calculate Non-configurational**  
**Contribution to Free Energy of Disorder in Magnetite**

Reference	$\alpha$ kJ mol <sup>-1</sup>	$\beta$ kJ mol <sup>-1</sup>	Entropy Term* J mol <sup>-1</sup> K <sup>-1</sup>
Ref. (1) fit to Ref. (26) data	$24.28 \pm 19.15$	$-23.00 \pm 19.15$	$-3.27 \pm 4.47$
Ref. 1 model	16.0	-20.0	$\sigma_{el} = -5.76$
Ref. (27)	$33.75 \pm 1.92$	$-26.36 \pm 1.34$	0
This work	$23.52 \pm 3.85$	$-32.66 \pm 2.58$	$(-0.625 \pm 0.091) \sigma^{mag} + \sigma_{el}$
(a) $\sigma_{el} = -0.41R$	$34.65 \pm 3.75$	$-38.11 \pm 2.51$	$(-0.563 \pm 0.089) \sigma^{mag} + \sigma_{el}$
(b) $\sigma_{el} = 0$	$50.66 \pm 3.65$	$-45.95 \pm 2.44$	$(-0.474 \pm 0.086) \sigma^{mag}$
(c) $\alpha = -(2/3)\beta$	20.68	$-31.02 \pm 1.05$	$(-0.664 \pm 0.075) \sigma^{mag} + \sigma_{el}^{**}$

\* Excludes configurational entropy.

\*\*  $\sigma_{el} = (-0.730 \pm 0.081) R$ .

Table III

**Octahedral Site Preference Energies and Disorder Entropies  
for Transition Metal Ions in Spinel Calculated from Energy Separation  
Between  $t_{2g}/e_g$  and  $e/t_2$  d-Electron Orbitals**

Ion	No. d Electrons	Crystal Field Stabilization*		$\Delta_{oct}$ kJ mol <sup>-1</sup>	OSPE kJ mol <sup>-1</sup>	$\sigma_{el}$ (tet)	$\sigma_{el}$ (oct)	$\sigma_{CFS} / R$ ** J mol <sup>-1</sup> K <sup>-1</sup>
		oct	tet					
Cr <sup>3+</sup>	3	12	8	187.8	158.6	R ln 3	0	1.099
Fe <sup>3+</sup>	5	0	0	-	0	0	0	0
Fe <sup>2+</sup>	6	4	6	124.4	16.6	R ln 2	R ln 3	-0.405
Co <sup>2+</sup>	7	8	12	116.0	30.9	0	R ln 3	-1.099
Ni <sup>2+</sup>	8	12	8	101.7	85.9	R ln 3	0	1.099
Cu <sup>2+</sup>	9	6	4	150.7	63.6	R ln 3	R ln 2	0.405
Zn <sup>2+</sup>	10	0	0	-	0	0	0	0

\* CFSE given in terms of  $\Delta/10$  where  $\Delta$  is the energy separation between either  $t_{2g}$  and  $e_g$  or  $e$  and  $t_2$  electron orbitals per Ref. (29). Note that  $\Delta_{tet} = (4/9) \Delta_{oct}$ .

\*\* Change in electronic entropy with disorder for ions in high spin state, per Ref. (1).

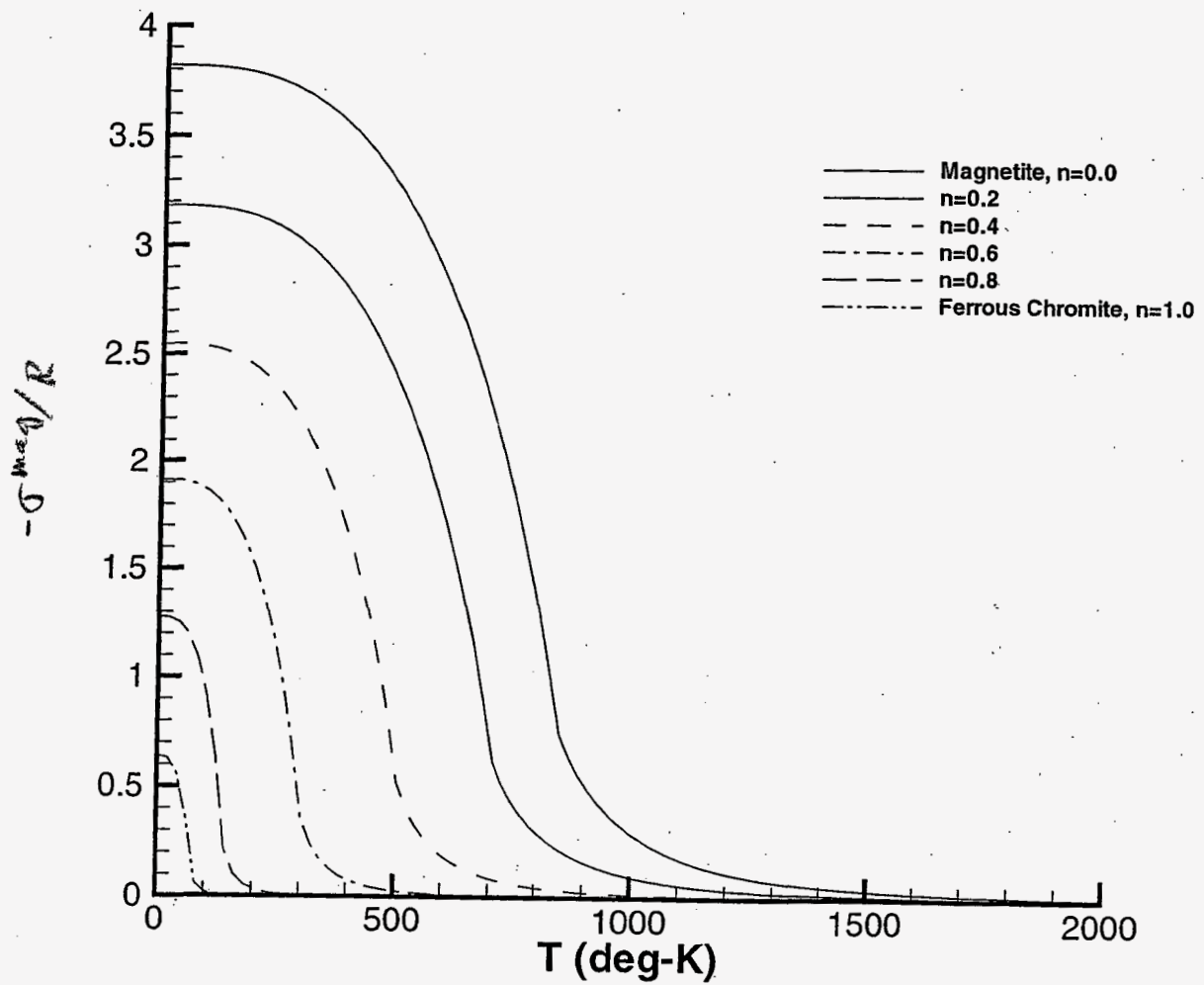


Fig. 1. Magnetic ordering contribution to entropy,  $\sigma^{\text{mag}}$ , in the  $\text{Fe}(\text{Fe}_{1-n}\text{Cr}_n)_2\text{O}_4$  spinel binary per Inden model.

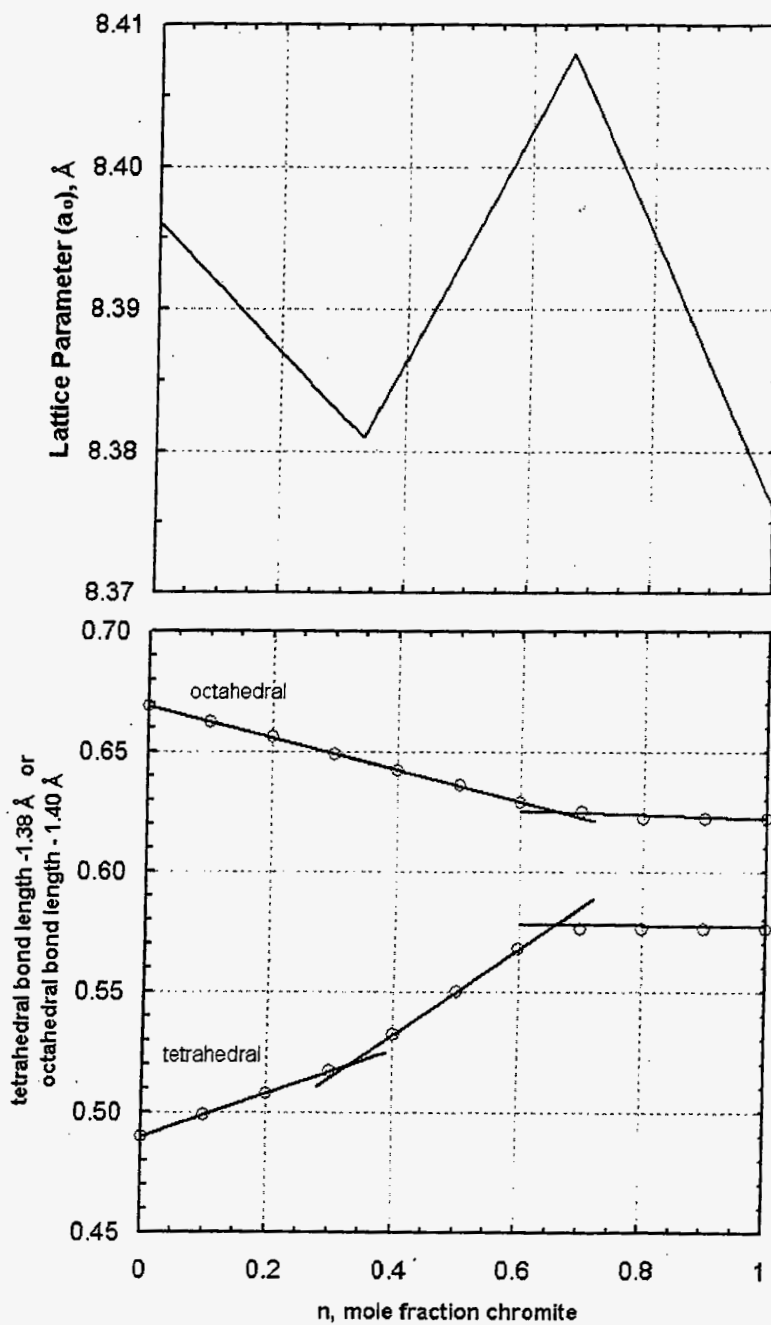


Fig. 2. M-O bond lengths inferred from spinel structure, lattice parameter and indicated cation distribution. Lattice parameter measurements shown in (a) are taken from Ref. 12.

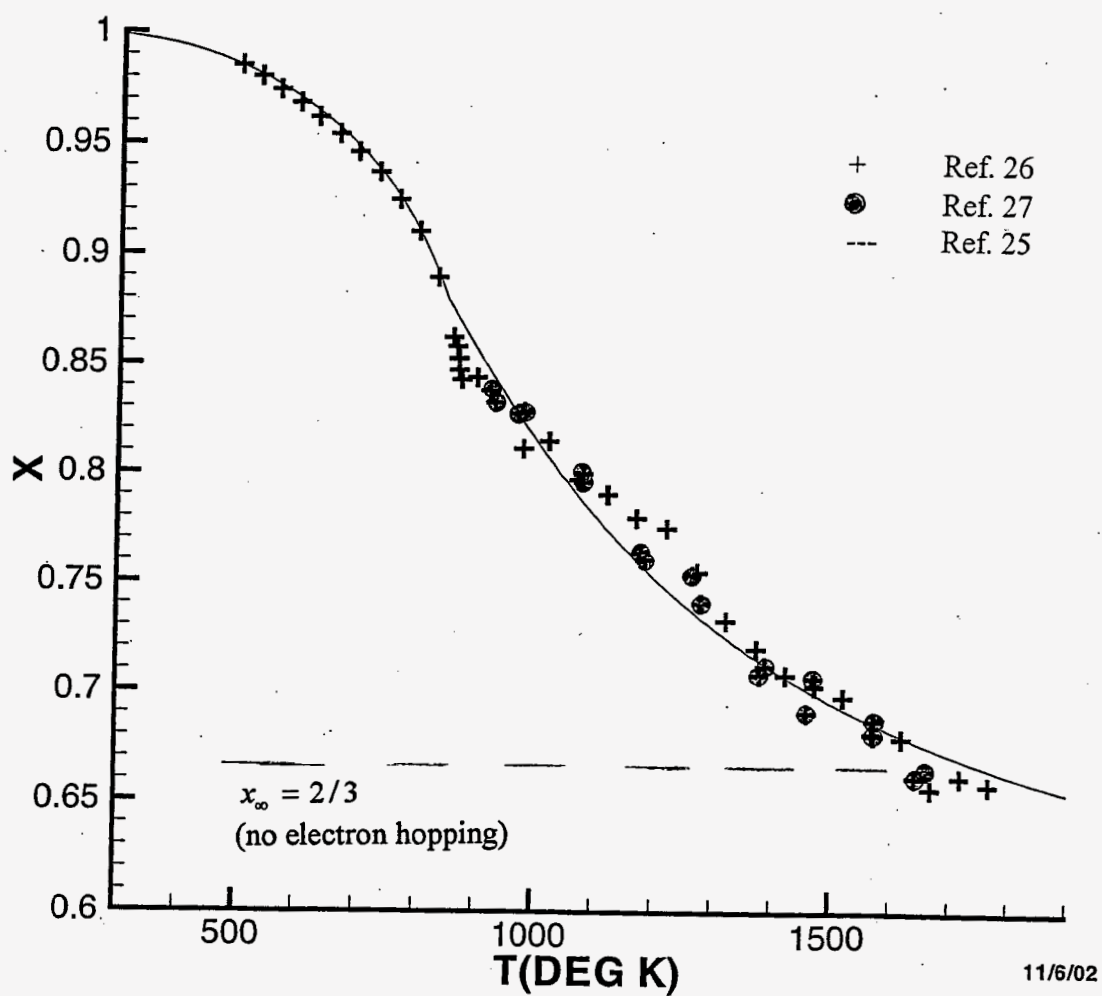


Fig. 3. Comparison of measured and fitted cation disordering parameter,  $x$ , in  $\text{Fe}_3\text{O}_4$ . Magnetite melts at 1870 K.



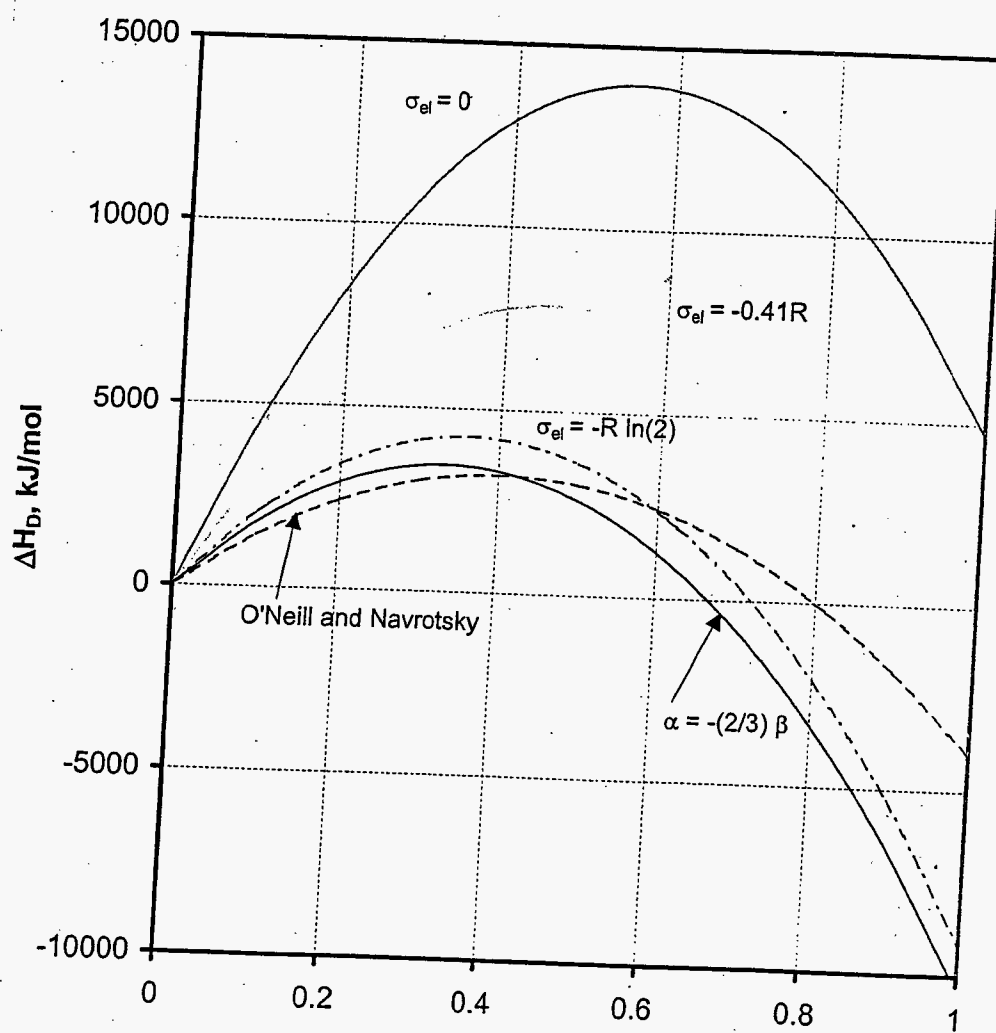


Fig. 4. Effect of  $\sigma_{el}$  constraint on enthalpies of disordering for magnetite,  $\Delta H_D$ .

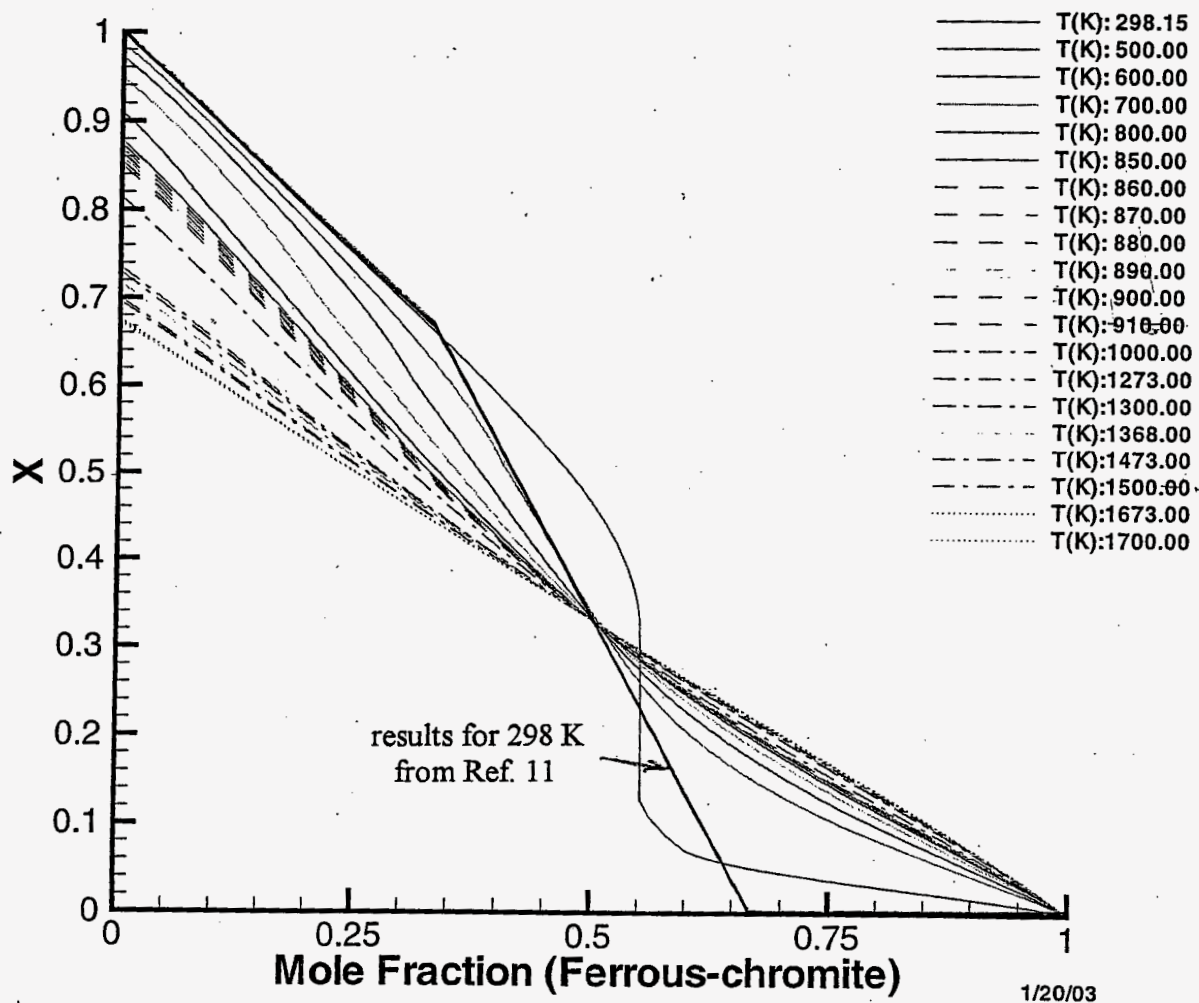


Fig. 5. Fraction of tetrahedral site  $\text{Fe}^{2+}$  ions disordered to octahedral sites in the  $\text{Fe}(\text{Fe}_{1-n}\text{Cr}_n)_2\text{O}_4$  spinel binary, accounting for configurational entropy changes due to electron hopping and coupling caused by alignment of magnetic moments of tetrahedral site  $\text{Fe}^{3+}$  ions vs. those of octahedral site  $\text{Fe}^{3+}$  and  $\text{Fe}^{2+}$  ions.

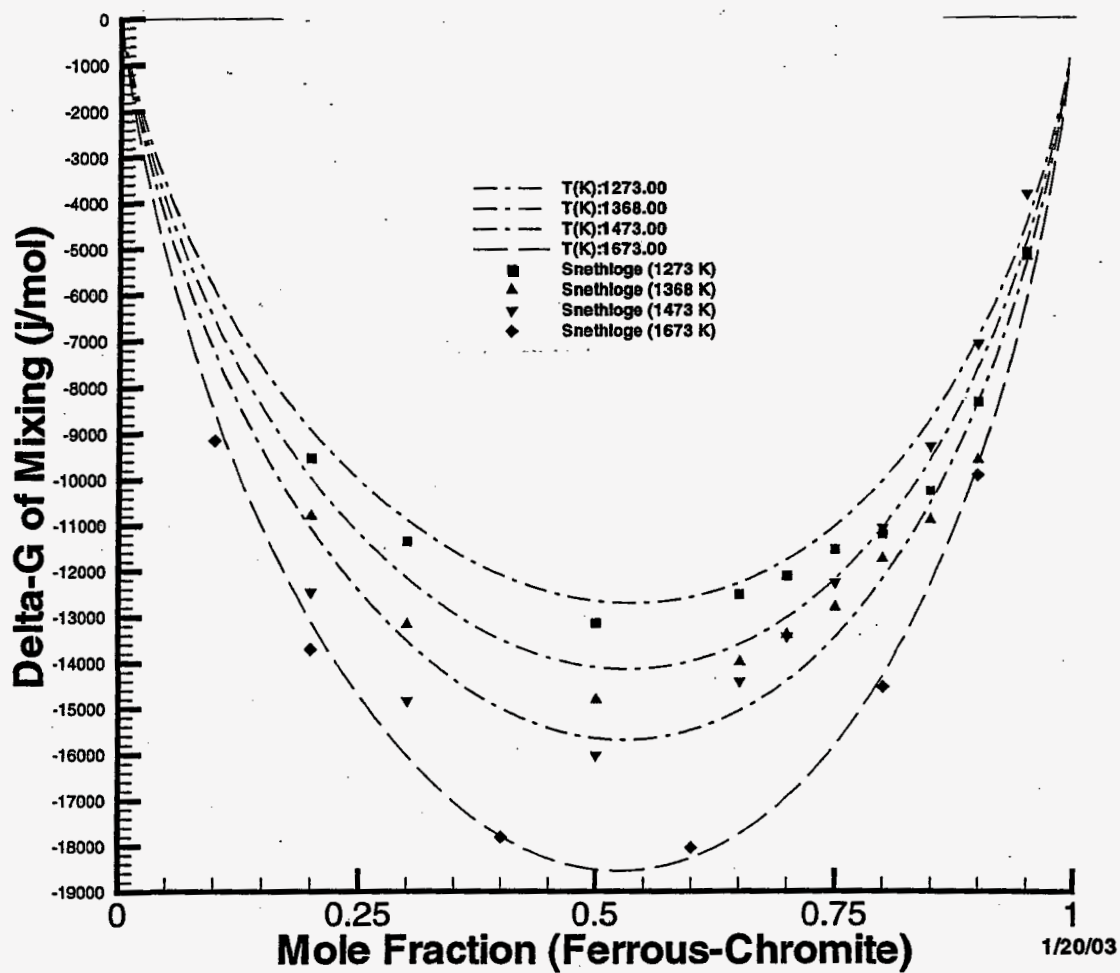


Fig. 6a. Comparison of measured and predicted free energies of mixing in the  $\text{Fe}(\text{Fe}_{1-n}\text{Cr}_n)_2\text{O}_4$  spinel binary. Data taken from Sneathlge and Schröcke ( $\square$  1273 K,  $\triangle$  1368 K and  $\nabla$  1473 K) and Petric and Jacob ( $\diamond$  1673 K).  $W = 6500 \text{ J mol}^{-1}$ ;  $\alpha$ ,  $\beta$ ,  $\gamma$  and  $\sigma_{el}$  obtained by regression of magnetite disordering data as discussed in text.

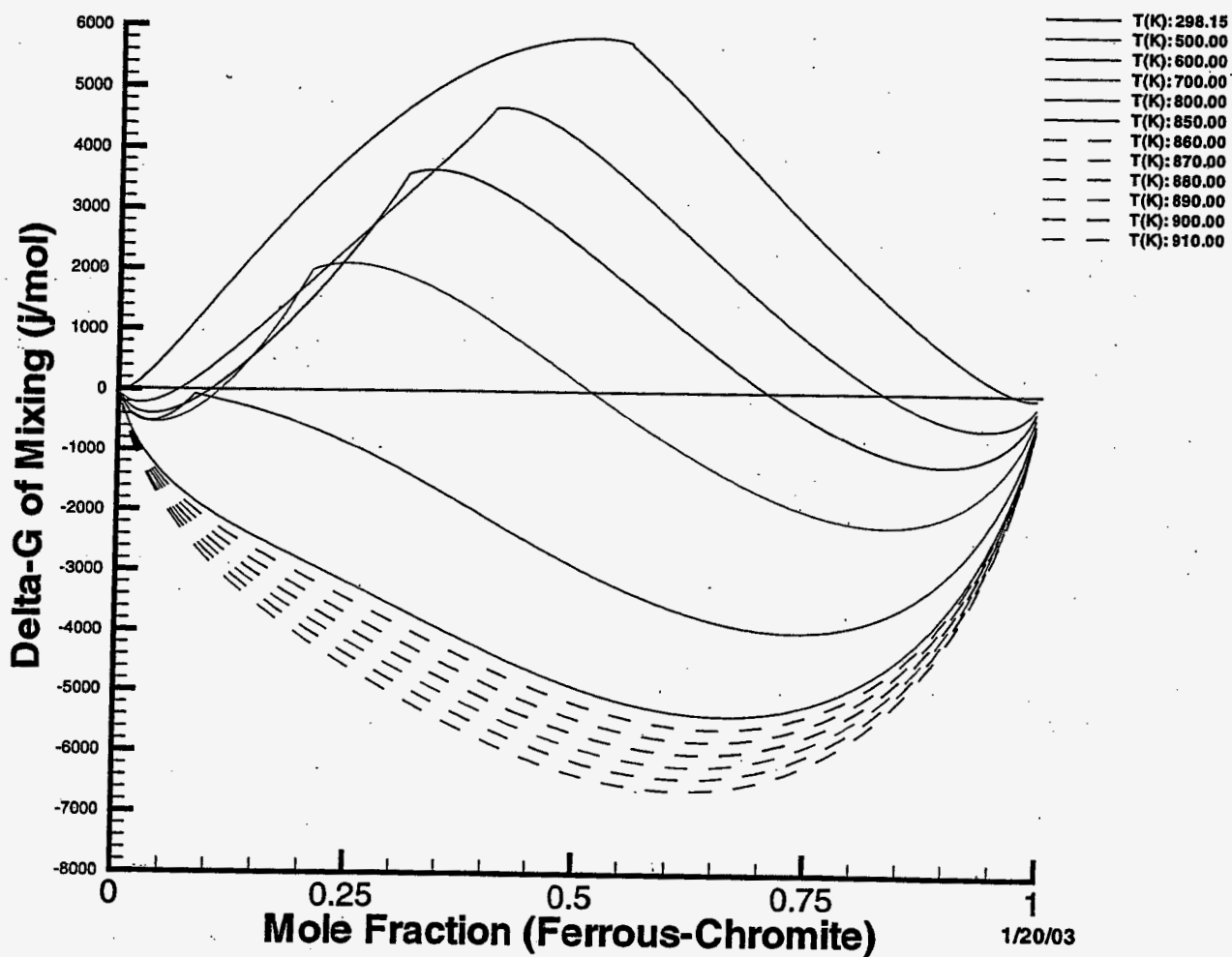


Fig. 6b. Predicted  $\Delta G_{mix}$  in  $Fe(Fe_{1-n}Cr_n)_2O_4$  spinel binary at temperatures below 1000 K. The discontinuity in slope of each  $\Delta G_{mix}$  curve below 800 K is an artifact of the Inden model and does not affect the solvus calculation, since it occurs in the two-phase region.

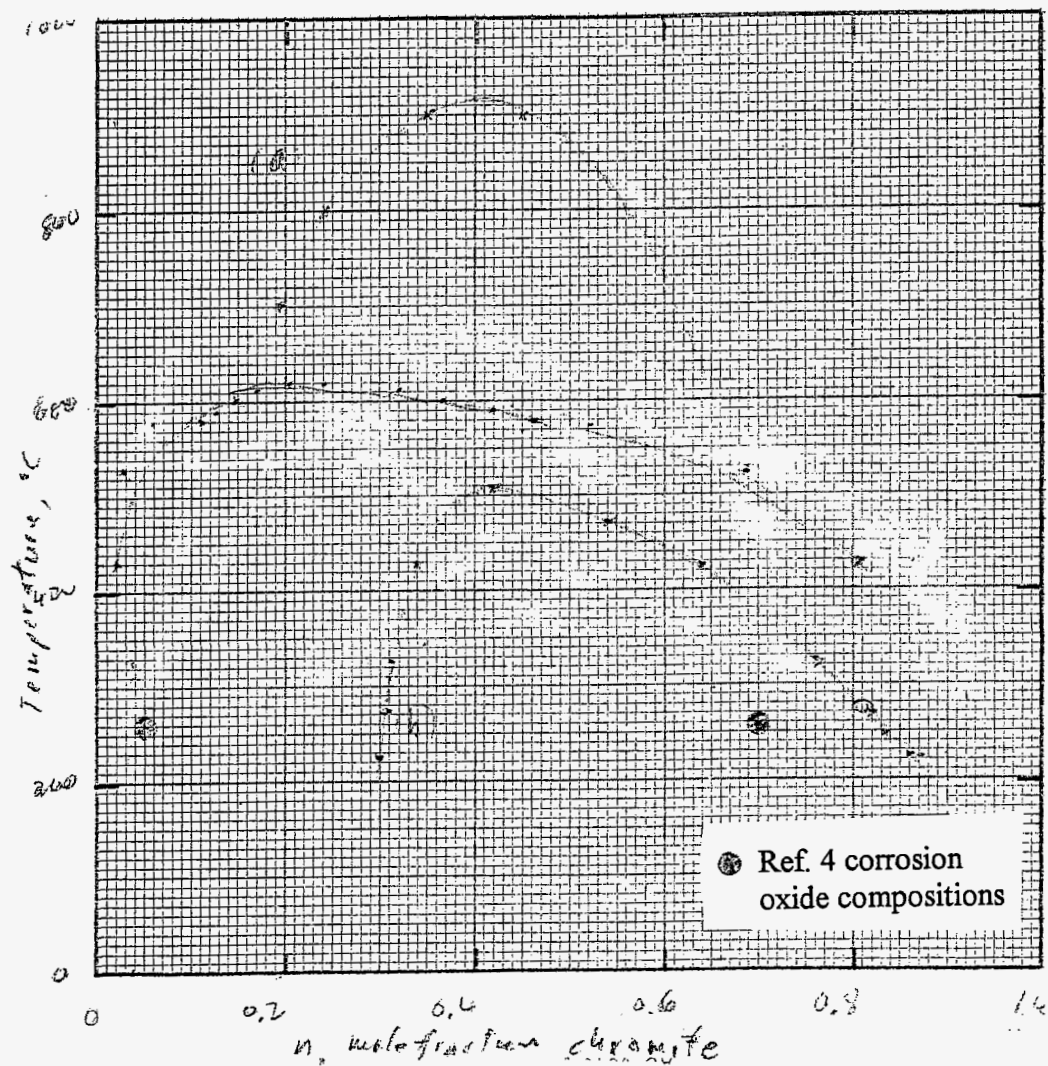


Fig. 7. Comparison of measured and predicted solvus in  $\text{Fe}(\text{Fe}_{1-n}\text{Cr}_n)_2\text{O}_4$  spinel binary: (a) Ref. 2 measurements, (b) Ref. 1 predictions, (c) revised predictions including magnetic ordering and electron hopping effects.